Initial ciliary assembly in *Chlamydomonas* requires Arp2/3-dependent recruitment from a ciliary protein reservoir in the plasma membrane

Brae M Bigge[1,2], Nicholas E Rosenthal[1,2], David Sept[3], Courtney M Schroeder[4], Prachee Avasthi[1,2]

[1]Biochemistry and Cell Biology Department, Geisel School of Medicine at Dartmouth College, Hanover, New Hampshire
[2]Anatomy and Cell Biology Department, University of Kansas Medical Center, Kansas City, Kansas
[3]Biomedical Engineering, University of Michigan, Ann Arbor, Michigan
[4]Division of Basic Sciences, Fred Hutchinson Cancer Research Center, Seattle, Washington

ABSTRACT

Cilia are organelles important for signaling and motility. They are composed of microtubules ensheathed in plasma membrane. The mechanisms related to ciliogenesis also require another cytoskeletal element, actin, which has been shown to be important for organizing the basal bodies and transition zone at the base of cilia and for short- and long-range trafficking. However, most studies of actin's role in ciliogenesis have taken a broad approach by knocking out all filamentous actin until now. Here, we more delicately dissect the interplay between actin and cilia by specifically focusing on actin networks nucleated by the Arp2/3 complex in *Chlamydomonas*. We find that knocking out Arp2/3-mediated actin networks dramatically impairs ciliary assembly and maintenance in these cells, and these defects are due to a problem with incorporation and gating of existing ciliary proteins, particularly in the early stages of assembly. We also show that cells lacking the Arp2/3 complex have more dramatic defects in ciliary maintenance using material from non-Golgi sources. Finally, we find relocalization of a ciliary membrane protein from the cell periphery to the cilia by internalization is dependent on actin and the Arp2/3 complex. Based on these results, we propose a new model of ciliary protein targeting during early ciliogenesis in which proteins previously targeted from the Golgi to the plasma membrane are reclaimed from this reservoir by Arp2/3-mediated networks.

INTRODUCTION

The microtubule-based cilium of the unicellular, green alga *Chlamydomonas reinhardtii* has long been used as a model due to its structural and mechanistic conservation relative to the cilia of mammalian cells. In fact, the cilia found on nearly every cell in the human body are remarkably similar to those found in *Chlamydomonas*, and like the cilia of *Chlamydomonas,* the cilia of human cells are also important for signaling and motility. Cilia consist primarily of microtubules that extend from the surface of the cell and are ensheathed in plasma membrane. Their assembly relies on microtubule dynamics and trafficking of protein and membrane (Nachury, Seeley, and Jin 2010), as well as intraflagellar transport (IFT), a motor-based transport system that moves tubulin and other cargo from the base of the cilium to the tip and back again (Pedersen and Rosenbaum 2008).

Although cilia are composed of microtubules and depend on them for assembly, the mechanisms governing ciliary maintenance and assembly extend to other cytoskeletal

components, such as actin. In mammalian cells, actin disruption results in increased ciliary length and percentage of ciliated cells (Kim et al. 2010; Park et al. 2008). In fact, the microtubule organizing center of the cell, the centrosome, from which cilia are nucleated has been found to function as an actin organizer (Farina et al. 2016; Inoue et al. 2019). Further, in mammalian cells, when ciliogenesis is triggered by serum starvation, preciliary vesicles are trafficked to the centriole where they fuse to form a ciliary vesicle around the budding cilium. It has been shown that when Arp2/3-branched actin is lost, depletion of preciliary vesicles at the centriole occurs, suggesting a role for branched actin in the initial steps of ciliogenesis in these cells (Wu, Chen, and Tang 2018). Actin itself has even been found within cilia, further suggesting that actin is a key protein involved in ciliary maintenance and assembly (Kiesel et al. 2020).

Chlamydomonas cells are an advantageous model due to their lack of a cortical actin network and their ability to undergo more consistent and robust ciliogenesis than mammalian cells without serum starvation. In *Chlamydomonas,* disruption of actin networks with Cytochalasin D (CytoD) resulted in shorter steady-state cilia (W. L. Dentler and Adams 1992), and disruption with Latrunculin B (LatB), which sequesters monomers leading to eventual filament depolymerization, resulted in shortened cilia and impaired regeneration (Avasthi et al. 2014; Jack et al. 2019). *Chlamydomonas* actin networks are required for accumulation of IFT machinery at the base of cilia and for entry of IFT material into cilia (Avasthi et al. 2014), as well as for trafficking of post-Golgi vesicles to cilia, the synthesis of ciliary proteins, and the organization of the gating region at the base of cilia (Jack et al. 2019). Many key advances in our understanding of the relationship between cilia and actin have been discovered using *Chlamydomonas,* which is proving to be a useful model for studying the actin cytoskeleton and its ciliary functions.

The actin cytoskeleton of *Chlamydomonas* contains two actin genes: *IDA5*, a conventional actin with 91% sequence identity to human β-actin; and *NAP1*, a divergent actin that shares only 63% of its sequence with human β-actin (Hirono et al. 2003; Kato-Minoura et al. 1998). We consider NAP1 to be an actin-like protein as opposed to an actin related protein (ARP) because it has a higher sequency identity when compared to actin than to conventional ARPs (**Supplemental Figure 1**), and because it is able to functionally compensate for the conventional filamentous actin (Jack et al. 2019; M. Onishi et al. 2018; M. Onishi, Pringle, and Cross 2016; Masayuki Onishi et al. 2019). Under normal, vegetative conditions the conventional IDA5 is the primary actin expressed, but when cells are treated with LatB, the LatB-insensitive NAP1 is upregulated (M. Onishi et al. 2018; M. Onishi, Pringle, and Cross 2016; Hirono et al. 2003). This separability of the two actins has led to the discovery that they can compensate for each other in ciliary maintenance and assembly (Jack et al. 2019). While knocking out IDA5 and NAP1 networks results in ciliary defects, studies of the role of actin in ciliary assembly have used global disruption by knocking out either one of the filamentous actins or both, yet actin networks have diverse compositions and topologies that lead to specific subfunctions within cells.

Actin networks rely on the actin binding proteins that contribute to the formation, arrangement, and function of the network. One such actin binding protein is the Arp2/3 complex, which nucleates branched or dendritic actin networks by nucleating a daughter filament off the side of an existing mother filament. The dendritic networks nucleated by the

Arp2/3 complex have been primarily found to be responsible for functions that involve membrane remodeling, for example lamellipodia and endocytosis (Campellone and Welch 2010).

Here, using the chemical inhibitor CK-666 to inhibit the nucleating function of Arp2/3 (Hetrick et al. 2013) and a genetic mutant of a critical Arp2/3 complex member, ARPC4 (Cheng et al. 2017; Li et al. 2019) we take a more delicate approach to investigating the role of actin in ciliary assembly by separating different actin networks into their expected subfunctions based on topology. Specifically, we probe the involvement of actin networks nucleated by the Arp2/3 complex in ciliary maintenance and assembly.

RESULTS

Arp2/3 complex nucleates diverse actin networks in *Chlamydomonas*:

The Arp2/3 complex from most eukaryotes consists of seven subunits: Arp2, Arp3, and ARPC1-5 (**Figure 1**), and each subunit plays a specific role of varying importance in the nucleation process. ARPC2 and ARPC4 form the core of the complex and the primary contacts with the mother filament, Arp2 and Arp3 serve as the first subunits of the daughter filament, and ARPC1 and ARPC3 play a role in nucleation but are not critical for branch formation (Robinson et al. 2001; Gournier et al. 2001). Each of these subunits are found in *Chlamydomonas* but have varying degrees of sequence homology compared with conventional Arp2/3 (**Figure 1**). Interestingly, the ARPC5 subunit has yet to be found in *Chlamydomonas*. ARPC5 is thought to be important for the association of ARPC1 to the complex, but a mammalian complex lacking ARPC5 and ARPC1 maintains some nucleating and branching activity and is able to cross-link actin normally (Gournier et al. 2001).

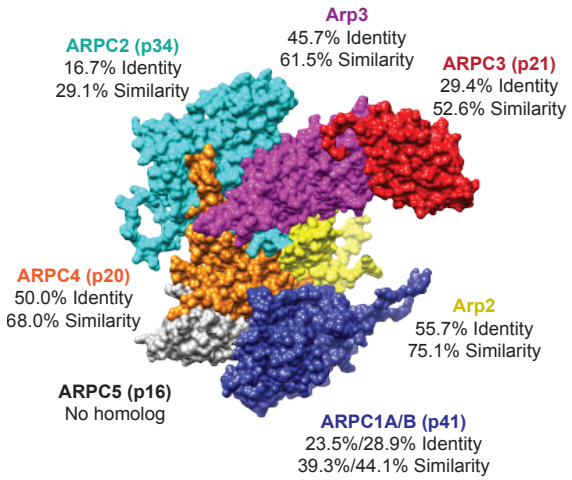

Figure 1. The actin-nucleating Arp2/3 Complex in *Chlamydomonas reinhardtii* lacks subunit ARPC5. Homology model of the *Chlamydomonas* Arp2/3 created using Modeller in UCSF Chimera and the template PDB: 1U2V, the bovine Arp2/3 complex. Percent identity and similarity is calculated in relation to the human Arp2/3 complex members. The bovine ARPC5 was placed in the model for reference, but the *Chlamydomonas* Arp2/3 genome lacks an ARPC5 subunit.

In order to determine the functionality of the Arp2/3 complex lacking ARPC5 in *Chlamydomonas*, we first looked directly at the effects of loss of Arp2/3 on the actin structures in the cell. For years, the visualization of filamentous actin in these cells has eluded researchers. However, recent advances from our lab have led to the ability to visualize the filamentous actin of vegetative *Chlamydomonas* cells using phalloidin (Craig et al. 2019).

Using these methods, we stained untreated wild-type cells and *arpc4* null mutants with phalloidin (**Figure 2A-B**). In normal, vegetative cells, a filamentous actin structure is observed in the middle of the cells, as well as apical spots around where cilia are docked (**Figure 2A-A'**). The *arpc4* mutant cells have a more condensed actin distribution in the middle of the cell with occasional bundles leading toward the base of the cilium (**Figure 2B-B'**). This was quantified two ways. First, line scans were taken through each cell from the apex between cilia to the farthest point on the basal surface (**Figure 2C-D**). Line scans show increased consistency and a more condensed nature of the actin signal in the *arpc4* mutants (**Figure 2C-D**). We further quantified this by fitting each line scan with a curve and uniformly measuring the width of the curves at half the maximum to show the width of the signal in the apical to basal plane (**Figure 2E**). This quantification shows that the *arpc4* mutants do indeed have a more condensed mid-cell actin in the axis measured (**Figure 2F**). We also quantified the ratio of the mid-cell actin area to the total cell area to determine if the actin signal of the *arpc4* mutant cells was more compact in all planes (**Figure 2G-H**). Mid-cell actin area was determined by uniformly thresholding all images so that only the actin signal in the mid-cell is visible. This quantification confirms *arpc4* mutant cells have a more compact mid-cell actin structure (**Figure 2H**). Furthermore, the actual intensity of the signal was found to be increased in the *arpc4* mutant cells (**Figure 2I**), while the fluorescence of the total cell, which was corrected for background fluorescence, is increased in the wild-type cells (**Figure 2J**).

Besides the actin signal seen in the mid-cell region of wild-type cells, apical dots are also typically seen near the base of cilia (**Figure 2A**). We quantified the presence of these dots in the wild-type cells compared to the *arpc4* mutant cells (**Figure 2K**). We found that while about 70% of wild-type cells contain the dots, hardly any (~5%) of the *arpc4* mutant cells had dots (**Figure 2K**). These results suggest that the Arp2/3 complex is involved in assembly of an actin-based structure at the base of the cilium, perhaps required for some sort of membrane remodeling.

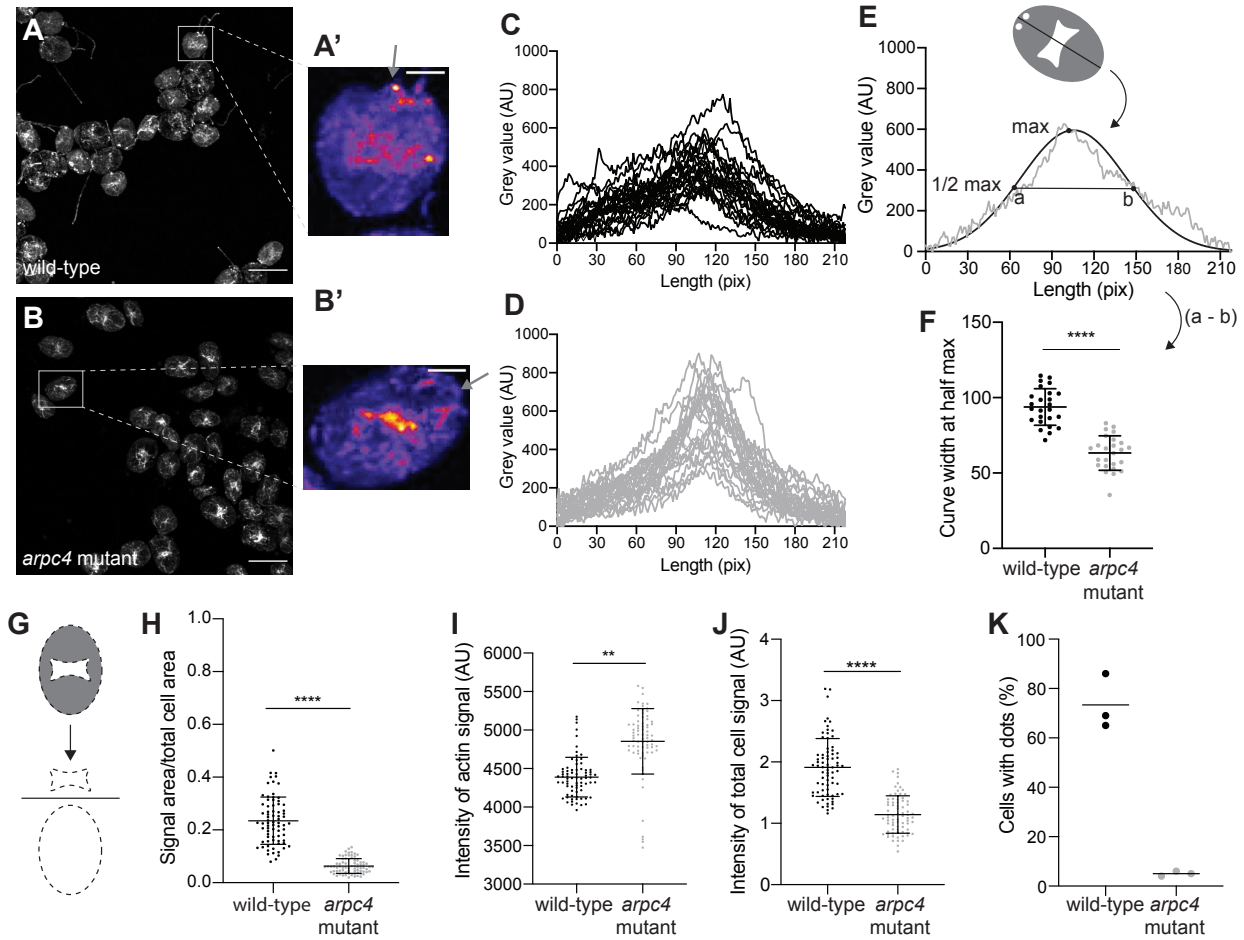

Figure 2. Loss of a functional Arp2/3 complex results in changes in actin distribution. A) Wild-type stained with phalloidin to visualize the actin network. Images were taken as a z-stack using spinning disk confocal imaging and are shown as a maximum intensity projection. Scale bar represents 10μm. **A'** shows the mid-cell actin network of the wild-type cells. The actin distribution is highlighted using the Fire LUT which highlights regions with the brightest intensity in yellow/orange and the areas with less intensity in blue. Grey arrow is pointing to the apex of the cell. Scale bar represents 2μm. **B)** *arpc4* mutant cells stained with phalloidin to visualize actin. Cells were imaged and are shown in the same way as A. Scale bar represents 10μm. **B'** shows lack of apical dots and the mid-cell actin staining of *arpc4* mutant cells. Image is shown in the same way as A'. Grey arrow is pointing to the apex of the cell. Scale bar represents 2μm. **C)** For wild-type cells, line scans were taken through the longest part of the cell from apical to basal. Background was subtracted and the length was normalized, then each line scan was plotted. n=25 for 3 separate experiments. **D)** For *arpc4* mutant cells, line scans were also taken through the longest part of the cell from apical to basal. Background was subtracted and the length was normalized, then each line scan was plotted in the graph. Note the width of the peaks and the consistency between the scans. n=25 for 3 separate experiments. **E)** Example of a line scan (grey) and fitted Gaussian curve (black) showing how to calculate the full width at half max shown in F. **F)** The full width at half max was calculated for the wild-type cells and the *arpc4* mutant cells based on line scans of C and D. Error bars represent standard deviation. n=25 for 3 separate experiments in each strain. P<0.001. **G)** Diagram demonstrating how the mid-cell actin/total cell actin was calculated in ImageJ. **H)** The ratio of mid-cell actin to total cell actin for wild-type and *arpc4* mutant cells. Error bars represent standard deviation. n=75 in 3 separate experiments for each strain. P=0.0002. **I)** The background-subtracted intensity of the mid-cell actin networks. Error bars represent standard deviation. n=75 for 3 separate experiments. P<0.01. **J)** Corrected total cell fluorescence of wild-type cells and *arpc4* mutant cells. Error bars represent standard deviation. n=75 in 3 separate experiments for each strain. P>0.0001. **K)** Percentage of cells with apical dots as shown in A'. Percentages taken from 3 separate experiments where n=100. P<0.0001.

Arp2/3 is required for the endocytosis-reminiscent relocalization of a membrane protein from the periphery of the cell to cilia:

The Arp2/3-dependent dots seen in *Chlamydomonas* resemble endocytic pits seen in yeast (Goode, Eskin, and Wendland 2015; Adams and Pringle 1984; Ayscough et al. 1997). Further, Arp2/3 is conventionally thought to be involved in endocytosis in cell-walled yeast to overcome turgor pressure (Aghamohammadzadeh and Ayscough 2009; Basu, Munteanu, and Chang 2014; Carlsson and Bayly 2014). *Chlamydomonas* cells also have a cell wall and since the apical actin dots resemble these endocytic pits, we hypothesized that Arp2/3 and actin-dependent endocytosis might be occurring in *Chlamydomonas* even though this process has not yet been directly demonstrated in this organism. We first investigated the presence of other proteins typically involved in different types of endocytosis (**Figure 3**). We compared the endocytosis proteins expressed in mammals and plants to those expressed in *Chlamydomonas*, and its closest relative, *Volvox carteri*. Both of the green algae were lacking the important machinery for almost all typical endocytosis processes, including caveolin for caveolin-mediated endocytosis, flotillin for flotillin-dependent endocytosis, and endophilin for endophilin-dependent endocytosis (**Figure 3**). However, most of the canonical clathrin-related endocytosis proteins could be found in both *Chlamydomonas* and *Volvox*, suggesting that clathrin-mediated endocytosis is conserved to a higher extent.

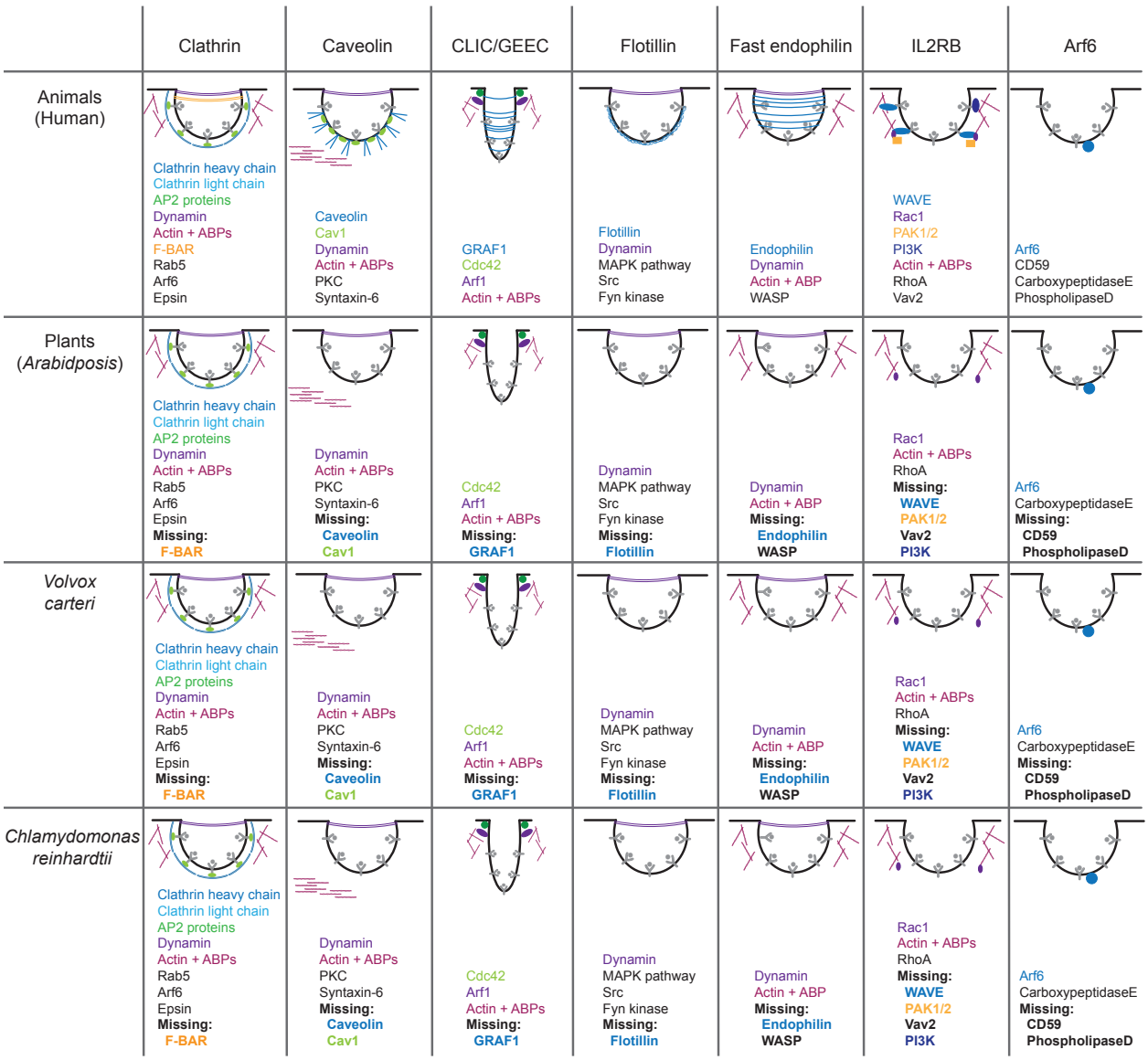

Figure 3. Comparison of endocytosis genes expressed in plants, animals, and 2 Green Algae. Presence of genes was determined using conventional mammalian genes and doing a BLAST search to identify similar genes in *Volvox carteri*, the closest relative of *Chlamydomonas,* and in *Chlamydomonas* itself. Colors of the words correspond to the color the protein represented in the diagrams.

We next determined the involvement of the Arp2/3 complex and actin in an endocytosis-reminiscent process by measuring the relocalization and internalization of a known ciliary protein. SAG1 is a membrane protein that relocalizes to cilia and is important for agglutination in mating *Chlamydomonas* cells (Belzile et al. 2013). When cells are induced for mating with dibutyryl-cAMP (db-cAMP), SAG1 must relocalize from the cell periphery to cilia, where it facilitates ciliary adhesion between mating cells. This relocalizaiton of SAG1 is thought to occur through internalization of the protein followed by internal trafficking on microtubules to the base of cilia (Belzile et al. 2013).

We examined whether actin and Arp2/3 were required for the transport of HA-tagged SAG1 to the apex of the cell and cilia for agglutination during mating (**Figure 4A**). Using immunofluorescence, we observed cells treated with either 10μM LatB to depolymerize IDA5 or 250μM CK-666 to perturb the Arp2/3 complex. Before induction SAG1-HA localized to the periphery of the cell (**Figure 4B**). 30 minutes after induction with db-cAMP, SAG1-HA relocalized to the apex of the cell and to cilia in untreated cells (**Figure 4B, left**). In both LatB and CK-666 treated cells, this apical enrichment was greatly decreased (**Figure 4B, middle and right**). To quantify this, line scans were drawn through the cell from the apex to the basal region (**Figure 4C-D**). The percentage of cells with apical enrichment was calculated, and it was found that untreated cells had a higher percent of apical enrichment when compared with LatB or CK-666 treated cells (**Figure 4E**). Thus, cells with perturbed Arp2/3-mediated filamentous actin show decreased efficiency of SAG1-HA relocalization.

We next asked if this decrease in efficiency of relocalization in cells with actin and Arp2/3 inhibition could be due to a decrease in the internalization of SAG1-HA through a process thought to be endocytosis. In order to investigate this, we used a method first described by Belzile et al. 2013, where cells were induced and treated with a low percentage (0.01%) of trypsin which will hydrolyze exterior proteins but cannot enter the cell. This assay allows us to determine the efficiency of internalization of SAG1-HA. In untreated cells, we see an increase in SAG1-HA protein levels following induction because SAG1-HA is internalized and becomes protected from trypsin (**Figure 4F**). In cells treated with either 10μM LatB or 250μM CK-666 we see a decrease in this trypsin protection as shown in the western blot (**Figure 4F**). This was further quantified by subtracting the amount of protein before induction from the amount of protein present after induction which gives a value representing the amount of SAG1-HA protected from trypsin due to induction in these cells (**Figure 4G**). The decrease in SAG1-HA following induction in cells with decreased filamentous actin and Arp2/3 complex function indicates a role for Arp2/3-mediated actin networks in internalization of a ciliary protein.

Finally, we tested endocytosis in these cells using the FM 4-46FX membrane dyes that are quickly endocytosed into cells showing bright foci within cells where dye is enriched in endocytosed compartments.. Wild-type and *arpc4* mutant cells were treated with these dyes and allowed to internalize dye for 1 minute. After a minute, cells were fixed and imaged. The background-corrected total cell fluorescence was calculated. Cells lacking a functional Arp2/3 complex have decreased total cell fluorescence (**Figure 4H-I**) suggesting they have decreased internalization of membrane in addition to protein.

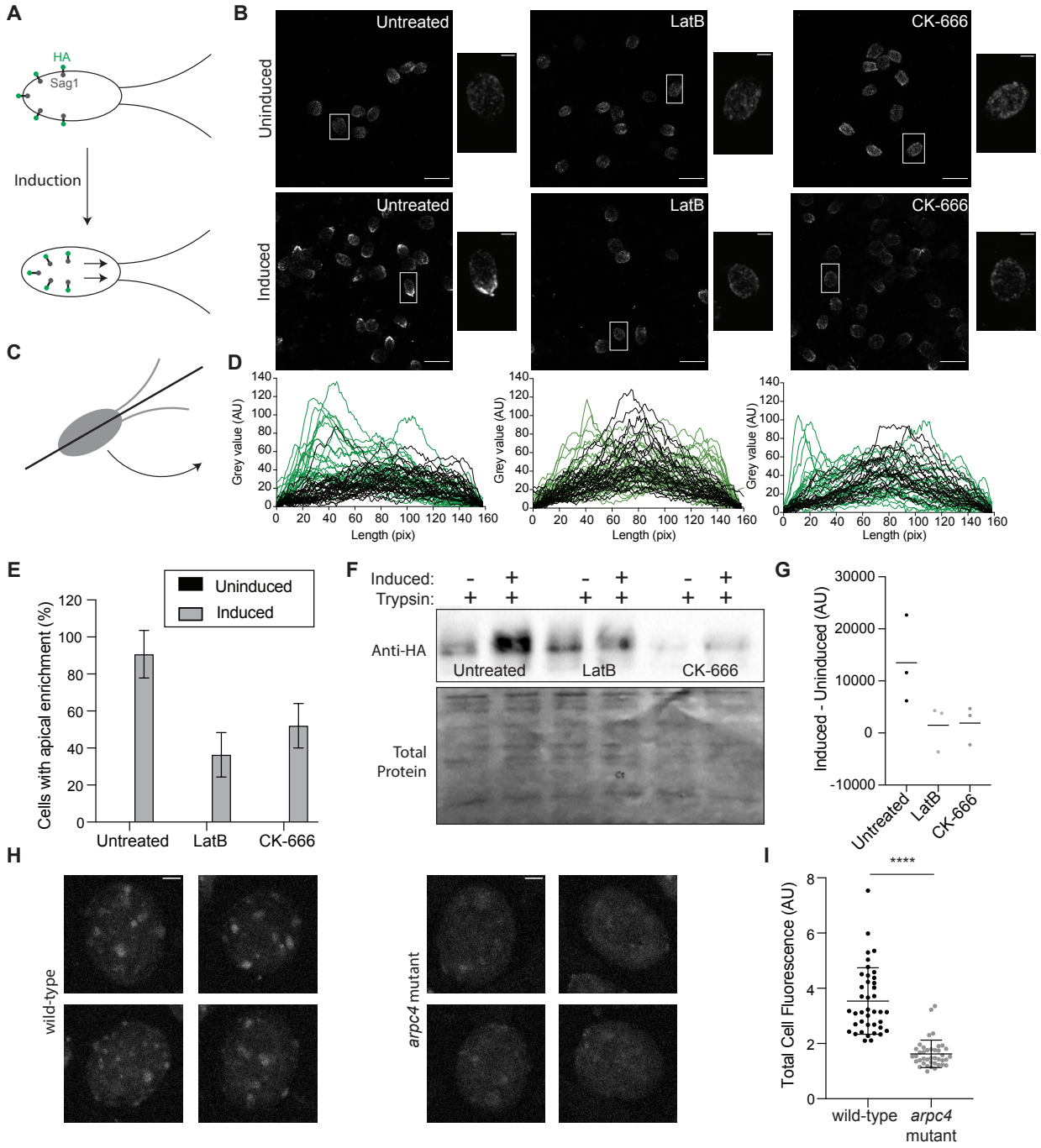

Figure 4. Arp2/3 is required for the relocalization and internalization of the ciliary protein SAG1 for mating. A) When mating is induced SAG1-HA is internalized and relocalized to the apex of the cells and cilia for agglutination. **B)** Maximum intensity projections of z-stacks taken using spinning disk confocal microscopy of SAG1-HA. Left is untreated, middle is treated with 10μM LatB, and right is treated with 250μM CK-666. Top row of images are uninduced and bottom row of images are induced with db-cAMP. Scale bar represents 10μm in full images and 2μm in the insets next to the images. **C)** Diagram representing line scans taken through the cells in z-stack sum images. **D)** Line scans for from the apex of the cell to the basal region of the cell in untreated cells (left), LatB treated cells (middle), and CK-666 (right). Black lines represent uninduced samples, green lines represent induced samples. **E)** Percentage of cells with apical enrichment based on E for uninduced (black) and induced (grey) cells for each treatment group. Error bars represent standard deviation. n=30 for 3 separate experiments for each treatment. **F)**

Western blot showing amount of SAG1-HA in uninduced and induced cells in each treatment group all treated with 0.01% trypsin. **G)** Intensity of the bands in H were normalized to the total protein as determined by amido black staining and quantified in ImageJ was used to subtract uninduced from induced to give a representation of the amount of SAG1-HA internalized with induction. N=3. **H)** FM 4-64FX is a membrane dye that is quickly endocytosed. Wild-type and *arpc4* mutant cells were treated with this dye and imaged on a spinning disk confocal. Maximum intensity projections of z-stacks are shown here. Scale bars represent 2μm. **I)** The background corrected total cell fluorescence was calculated for membrane dye treated cells. Error bars represent standard deviation. n=30 for 3 separate experiments. P<0.0001.

Loss of Arp2/3 inhibits normal regeneration and maintenance of cilia:

Knowing the roles of the Arp2/3 complex in maintaining actin distribution and in ciliary protein internalization, we asked what specific functions these networks had in ciliary assembly. We first investigated the requirement for Arp2/3 in maintenance of cilia by treating cells with either 100μM CK-666, 250μM CK-666, or the inactive control CK-689 (250μM) for 2 hours and looking at the effect on steady state ciliary length. Consistent with previous results (Avasthi et al. 2014), we found that treating cells with CK-666 created a decrease in ciliary length, suggesting that Arp2/3 is required for maintaining cilia (**Figure 5A**). We saw no changes in ciliary length with the inactive CK-689 (**Figure 5A**) or when *arpc4* mutant cells were treated with CK-666 (**Supplemental Figure 2**). However, untreated *arpc4* mutants do have a decreased ciliary length when compared with wild-type cells (**Figure 5B**) again suggesting Arp2/3 is required for normal ciliary length maintenance.

Next, we investigated the requirement for Arp2/3-nucleated actin in the more complicated process of ciliary assembly where there is a high demand for protein and membrane both from pools of protein already existing in the cell and from new protein synthesis (Wingfield et al. 2017; Nachury, Seeley, and Jin 2010; Rohatgi and Snell 2010; Jack et al. 2019; Diener, Lupetti, and Rosenbaum 2015). In order to investigate assembly, cells were deciliated by low pH shock and then allowed to synchronously regenerate cilia after being returned to normal pH (Paul A. Lefebvre 1995). We found that cells lacking a functional Arp2/3 complex were slow to regenerate their cilia, and in fact, two-thirds of cells did not regrow cilia at all (**Figure 5C**). Importantly, the initial steps are the slowest portion of assembly.

This result is puzzling because the loss of Arp2/3 results in a more dramatic phenotype than that of the *nap1* mutants treated with LatB, which are lacking all filamentous actins (Jack et al. 2019). However, in the *arpc4* mutant cells, a functional Arp2/3 complex never exists and therefore, they never have Arp2/3-mediated actin networks. In *nap1* mutant cells treated with LatB, the treatment begins shortly after deciliation causing an acute perturbation. Further, LatB functions by sequestering actin monomers to promote filament disassembly, and thus the effects may not be immediate (Spector et al. 1989). Therefore, it is likely that there is a brief window where actin can assert its initial role in ciliary regeneration before being depolymerized. To avoid this, we began the LatB treatment in *nap1* mutants 30 minutes before deciliation. This pre-treatment allows us to observe what happens when actin is not present immediately after deciliation. (**Figure 5D-E**). In this case, we see decreased ciliary length and dramatically decreased percent ciliation, which is consistent with our *arpc4* mutant results.

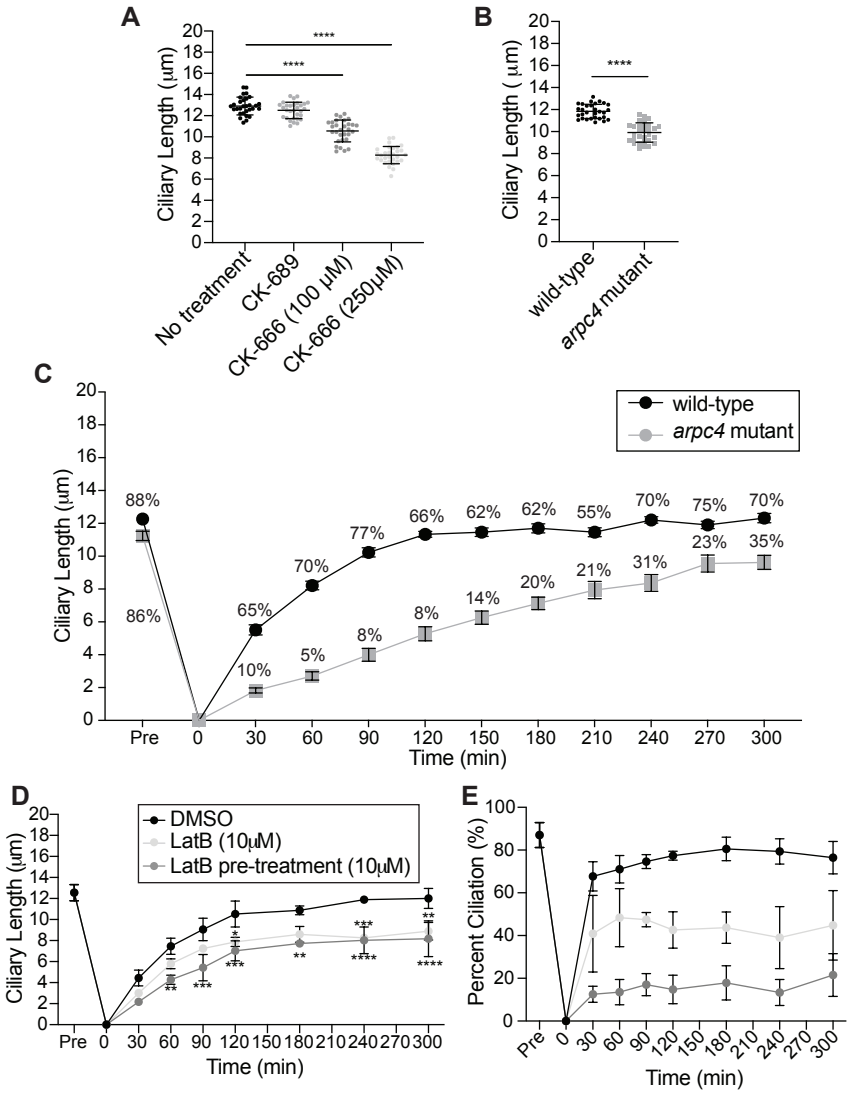

Figure 5. Arp2/3 is required for normal ciliary maintenance and assembly. A) Wild-type cells were treated with 100µM or 250µM of CK-666 or the inactive CK-689 for 2 hours. Cells were then imaged using a DIC microscope and cilia were measure in ImageJ. Error bars represent standard deviation. n=30 for each treatment in 3 separate experiments. P<0.0001. **B)** Wild-type cells and *arpc4* mutant cells steady state cilia were also measured with no treatment. Error bars represent standard deviation. n=30 for each strain for 3 separate experiments. P<0.0001. **C)** Wild-type cells and *arpc4* mutant cells were deciliated using a pH shock and then allowed to regrow. The black line represents wild-type, while the grey line represents the *arpc4* mutant. The numbers above or below each point show the percent ciliation for the wild-type and *arpc4* mutant cells respectively. Error bars represent 95% confidence interval. n=30 for each strain and each time point in 3 separate experiments. For every time point except 0 min, P<0.0001 in terms of both length and percent ciliation. **D)** Wild-type cells were pre-treated with 10µM LatB for 30 minutes before deciliation or treated with LatB upon the return to neutral pH following deciliation. The black line represents untreated cells, while the light grey line represents cells treated with LatB following deciliation and the dark grey line represents cells pre-treated with LatB. Error bars represent standard deviation. N=3 separate experiments. For every time point except 0 min. *P<0.1, **P<0.01, ***P<0.001, ****P<0.0001. Asterisks for the pretreatment are located below the graph, while asterisks for the post treatment are located above the line. **E)** Percent ciliation for the experiment in E. Line color is the same as E. Error bars represent standard deviation.

Arp2/3 is required for the incorporation of existing membrane and proteins for ciliary assembly:

There are several distinct steps of ciliary assembly after severing, all of which require actin filaments. The first step requires that a pool of existing proteins are incorporated into cilia in an actin-dependent manner (Jack et al. 2019). The finding that Arp2/3-mediated actin networks result in slow initial ciliary assembly, when it is likely that existing protein is being incorporated, led us to question the involvement of Arp2/3-dependent actin networks in the incorporation of existing ciliary protein.

By treating regenerating cells with cycloheximide, a protein synthesis inhibitor, we can eliminate two steps of the process of ciliary assembly (**Figure 6A**) (Rosenbaum, Moulder, and Ringo 1969). Without protein synthesis, there is no trafficking or incorporation of new proteins. Therefore, any ciliary growth we see is due to the incorporation of the existing protein alone. Under normal conditions, cells that are deciliated and treated with cycloheximide typically grow to about half-length, or 6μm, within 2 hours (**Figure 6B**). We also saw cells growing to half-length after 2 hours when treated with the inactive CK-689 and cycloheximide (**Figure 6B**). However, when treated with either 100μM or 250μM CK-666 and cycloheximide, cells exhibit a dose-dependent decrease in ciliary length after 2 hours of regeneration (**Figure 6B**).

To confirm the results of chemical perturbation, we used the *arpc4* mutant strain to genetically test the role of Arp2/3 in incorporation of existing protein. When *arpc4* mutant cells were deciliated and treated with cycloheximide, they barely show any growth at all (**Figure 6C**). In fact, throughout a five-hour period, we never saw above 6% of cells with cilia (**Figure 6C**). This suggests that the Arp2/3 complex and the actin networks nucleated by the complex are indispensable for the incorporation of existing protein in ciliary assembly. However, we have not ruled out that the normal excess of ciliary proteins may be affected in *arpc4* mutant cells.

To investigate why loss of Arp2/3 results in incorporation defects, we turned to the transition zone, the region at the base of cilia responsible for gating (Szymanska and Johnson 2012). We observed the localization of a known transition zone protein, NPHP4 (Awata et al. 2014). In wild-type cells, NPHP4 localizes in two dots at the base of cilia (**Figure 6D-E**). When cells are treated with LatB for a short period of time (30 minutes), the conventional actin IDA5 depolymerizes and the localization of NPHP4 is lost (**Figure 6D-E**) (Jack et al. 2019). After 2 hours, the divergent actin NAP1 is upregulated and the localization of NPHP4 is restored (**Figure 6D-E**) (Jack et al. 2019). When cells are treated with LatB to disrupt the conventional actin network and with CK-666 to prevent Arp2/3 nucleation, the NAP1-dependent restoration of NPHP4 localization is blocked (**Figure 6D-E**), suggesting Arp2/3 is required for the organization of the transition zone particularly when it relies on the divergent actin, NAP1. This led us to question whether Arp2/3 could interact with the divergent actin.

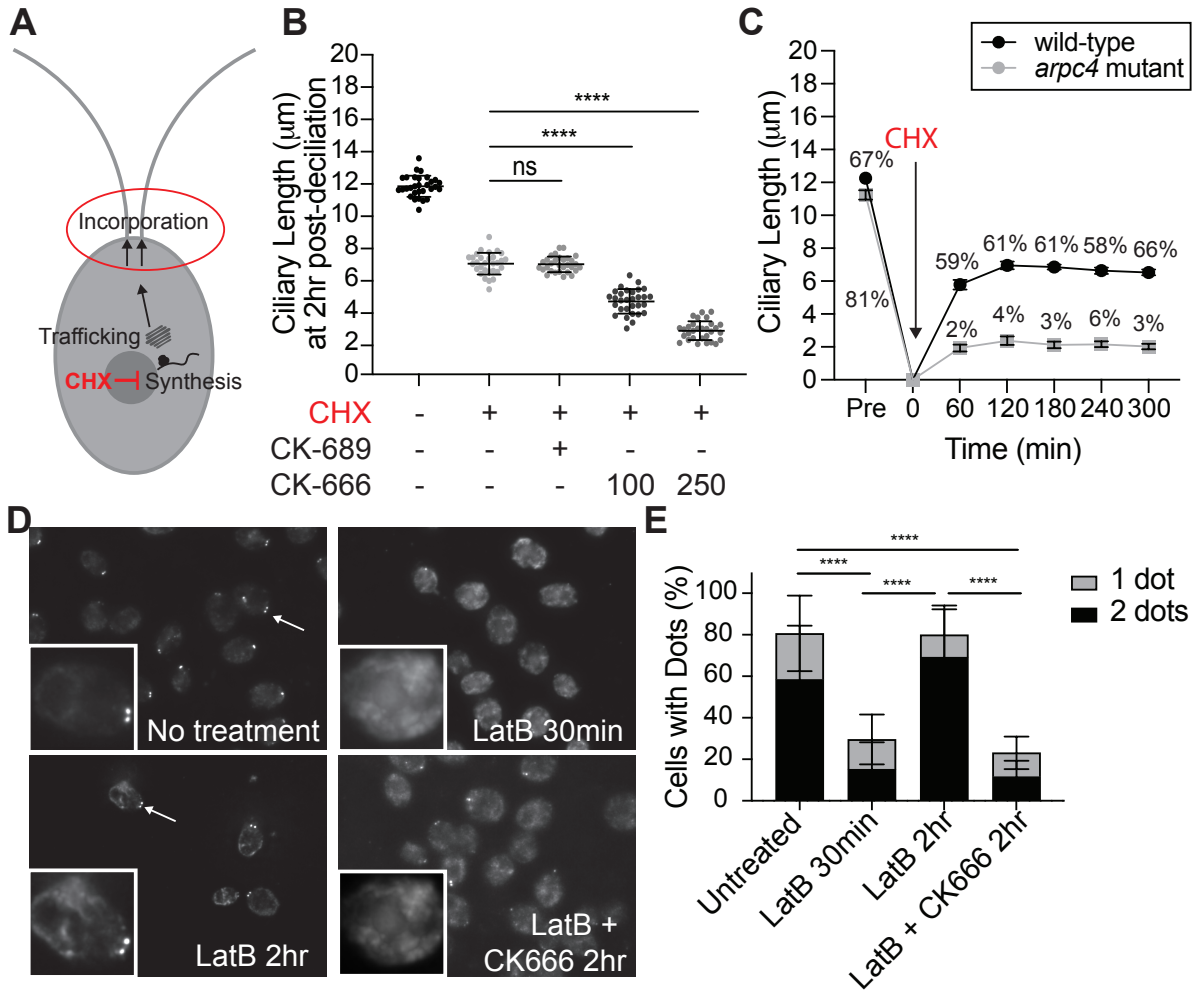

Figure 6. Arp2/3 is required for incorporation of existing protein during ciliary assembly. A) Treating cells with cycloheximide stops protein synthesis, which means only incorporation of existing protein is observed. **B)** Wild-type cells were deciliated and then treated with a combination of 10µM cycloheximide (CHX) and CK-666 (100µM or 250µM) or CK-689 (the inactive control) at the same concentration during regrowth. The graph shows the length of their cilia after 2 hours of treatment and regrowth. Error bars represent standard deviation. n=30 for each treatment group at each time point in 3 separate experiments. For both the 100µM and 250µM CK-666 treatments with CHX, P<0.0001. **C)** Wild-type cells and *arpc4* mutants were deciliated and then allowed to regrow in 10µM CHX. The percentages above the lines represent the percent of cells with cilia at the indicated time points. Error bars represent 95% confidence interval. n=30 for each strain and each time point in 3 separate experiments. For every time point besides 0 min, P<0.0001 for both length and percent ciliation. **D)** Maximum intensity projections of deconvolved widefield immunofluorescence images of NPHP4-HA. Arrows point to localization of NPHP4-HA at the base of cilia. **E)** Percentage of cells with either 1 apical dot (grey) or 2 (black) representing NPHP4 localizing to the base of cilia. Error bars represent standard deviation. n=100 for each sample in 3 separate experiments. **** represents P<0.0001.

Arp2/3 interacts with both IDA5 and NAP1 despite sequence divergence:

The actin cytoskeleton of *Chlamydomonas* is unique in that it has 2 very different actins: IDA5, a conventional actin, and NAP1, a divergent actin (Hirono et al. 2003; Kato-Minoura et al. 1998; M. Onishi, Pringle, and Cross 2016). The region of actin on the mother filament that binds

ARPC2 and ARPC4 (Goley et al. 2010), the core of the Arp2/3 complex, is well-conserved in IDA5. However, this region in NAP1 is quite divergent with only 43% of the 30 residues thought to bind ARPC2 and ARPC4 conserved in NAP1. This leads us to hypothesize that Arp2/3 can interact with IDA5 normally but not with NAP1 (**Figure 7A-B**).

Despite the sequence divergence, previous work from our lab has found that the two actins function redundantly in ciliary assembly (Jack et al. 2019). This led us to question whether the two actins could interact with Arp2/3 for actin-dependent ciliary maintenance and assembly functions. We answer this question using the *nap1* null mutant that only contains IDA5 and the *ida5* null mutant that only contains NAP1 (Kato et al. 1993; Kato-Minoura, Hirono, and Kamiya 1997). In this assay, cells are treated with an inhibitor, and because intact actin filaments are required to maintain cilia, the ciliary length can be used as a readout of actin network integrity. This is illustrated in the case of LatB (Avasthi et al. 2014). When wild-type cells containing both IDA5 and NAP1 are treated with LatB, cilia shorten but are able to restore their length. This is because NAP1 is upregulated and resistant to LatB, and therefore, can compensate for the lost IDA5. When *nap1* mutant cells containing only IDA5 are treated with LatB, cilia shorten because NAP1 is not present to compensate for depolymerized IDA5. When *ida5* cells containing only NAP1 are treated with LatB, there is no effect as NAP1 is insensitive to LatB (**Figure 7C**) (Avasthi et al. 2014). We modified this assay by treating wild-type cells, *nap1* mutants, and *ida5* mutants with the Arp2/3 inhibitor CK-666 or the inactive CK-689. Unlike what was seen with LatB, which affects NAP1 and IDA5 differently, we found that in all three strains, cilia of cells treated with CK-666 shorten, so inhibiting Arp2/3 affects cells that express either actin (**Figure 7C**). Thus, Arp2/3 may interact with both IDA5 and NAP1 to maintain ciliary length despite the sequence divergence of NAP1 in the Arp2/3 binding region.

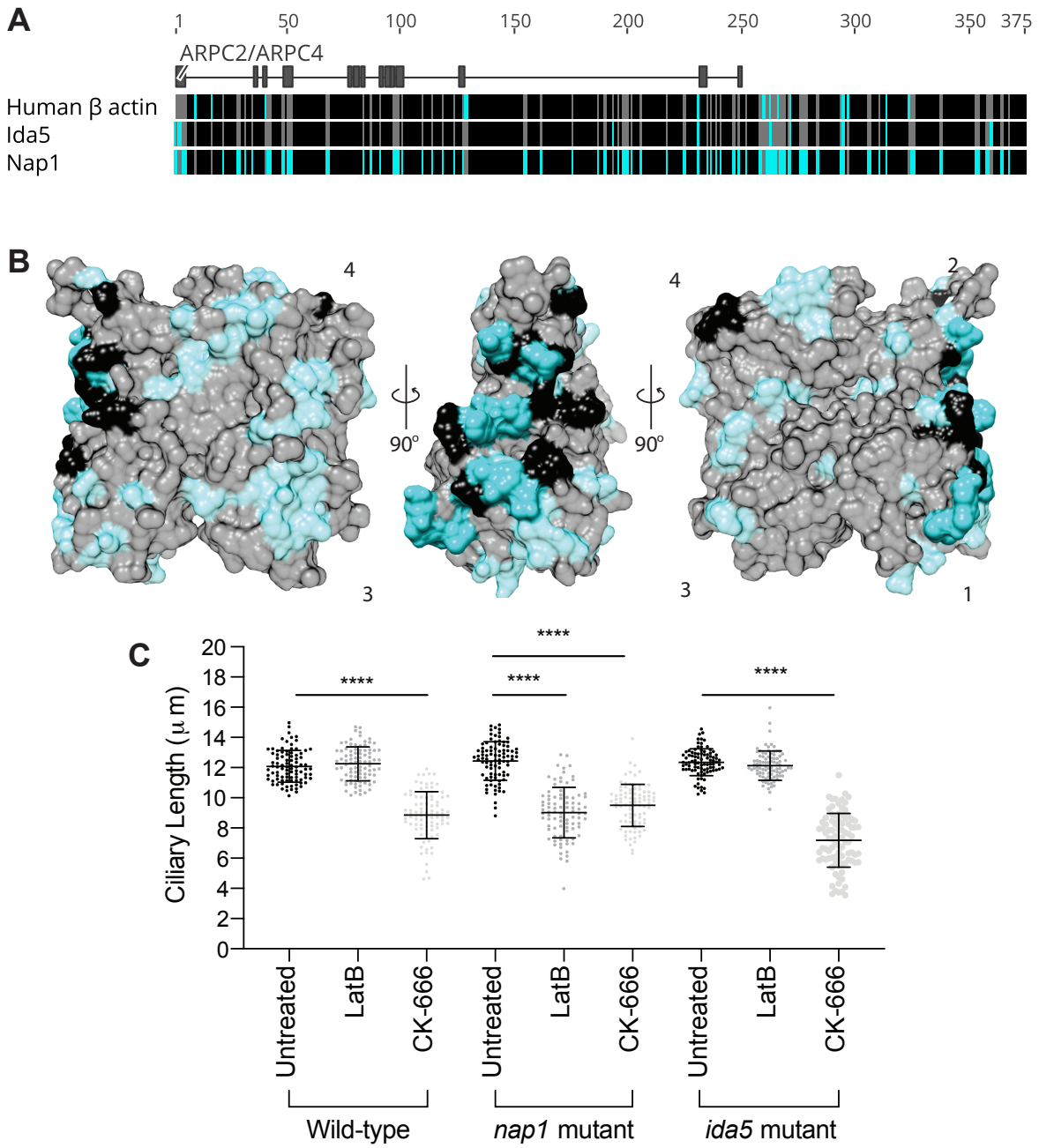

Figure 7. Arp2/3 interacts with both IDA5 and NAP1 despite sequence divergence. A) Conservation map based on the sequence alignment between IDA5, NAP1, and human actin generated in Geneious using MUSCLE. Black residues are conserved, grey residues are similar, and cyan residues are divergent. The regions of actin that bind ARPC2/ARPC4 are annotated above the alignment, with grey bars connected by lines. 43% of residues that interact with Arp2/3 are conserved in NAP1. The full alignment containing IDA5 and NAP1 with human actin and actin related proteins can be found in Supplemental Figure 1. **B)** Homology model of IDA5 based on the structure PDB 2ZWH with conservation of NAP1 mapped on the surface. Grey (transparent) residues are conserved between IDA5 and NAP1, while cyan residues are divergent. The darker cyan and black regions (non-transparent) interact with ARPC2/ARPC3, while the more transparent regions do not. **C)** Wild-type cells, *nap1* mutant cells, and *ida5* mutant cells were treated with either LatB, CK-666, or the inactive CK-689 (Supplemental Figure 2A) for 2 hours and then cilia were measured. Error bars represent standard deviation. n=30 for each treatment and each strain in three separate experiments. **** represents P<0.0001.

Cilia of Arp2/3 mutant cells collapse in the absence of the Golgi:

Because we see defects in ciliary assembly and maintenance when cells are likely incorporating existing protein we wanted to tease apart the mechanism that is perturbed when Arp2/3 is lost. Arp2/3 is canonically thought to be involved in membrane remodeling functions, so we were interested in investigating membrane delivery to cilia. The Golgi is known to be the main source of membrane for cilia (Nachury, Seeley, and Jin 2010; Rohatgi and Snell 2010). In *Chlamydomonas,* this has been demonstrated by the ciliary shortening of cells treated with Brefeldin A (BFA), a drug that causes Golgi collapse (W. Dentler 2013). In order to determine if Arp2/3 is involved in the trafficking of new protein from the Golgi to cilia, we looked at the Golgi following deciliation using transmission electron microscopy (TEM) (**Supplemental Figure 3A**). The Golgi appeared grossly normal, and in all cases had approximately the same number of cisternae (**Supplemental Figure 3A-B**). However, alternative pathways for ciliary material have also been found by biotinylating the surface proteins and then deciliating the cells, meaning the membrane and proteins within cilia were lost. When cilia were allowed to regrow, biotinylated proteins were found to reside within the new cilia suggesting they came from the plasma membrane (W. Dentler 2013). Therefore, we hypothesized that due to its role in membrane remodeling, and particularly endocytosis, Arp2/3 is part of an endocytic pathway that provides membranes and perhaps membrane proteins to cilia (**Figure 8A**). In order to test this, we treated cells with 36µM BFA, so that Golgi-derived membrane would no longer be available, and cells would be forced to utilize other sources of ciliary proteins and membranes. Wild-type cells treated with BFA resorb slowly, but *arpc4* mutant cells had a faster speed of resorption (**Figure 8B and D**). Further, the number of cells with cilia in the *arpc4* mutant cells dramatically decreases with BFA treatment (**Figure 8C**). Additionally, cells treated with known-ciliary resorption-inducing drugs, 3-isobutyl-1-methylxanthine (IBMX) (Pasquale and Goodenough 1987) or sodium pyrophosphate (NaPPi) (P. A. Lefebvre et al. 1978) resorb cilia through a different mechanism and do not show this change in velocity (**Supplemental Figure 4**). Thus, cells lacking Arp2/3 have a higher reliance on the Golgi for ciliary membrane and protein, which suggests an alternative route of membrane and protein delivery in wild-type cells.

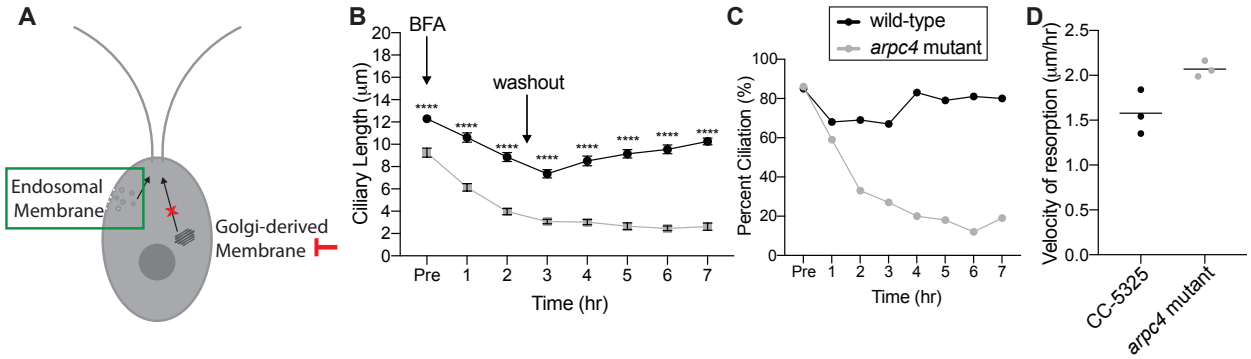

Figure 8. Arp2/3 is required for ciliary maintenance in the absence of intact Golgi. A) Diagram of hypothesis being tested and potentially what occurs in BFA treatment. **B)** Cells were treated with 36µM BFA for 3 hours at which time the drug was washed out. Wild-type is represented by black, while *arpc4* mutants are grey. Error bars represent 95% confidence interval. n=30 for each time point and each strain in 3 separate experiments. **** represents P<0.0001. **C)** Percent ciliation of the cells in B. n=100. **D)** Resorption speed for wild-type cells and *arpc4* mutant cells as

determined by fitting a line to the first 4 time points before washout and determining the slope of the line. N=3. P>0.0001.

DISCUSSION

In this study, we introduce the Arp2/3 complex of *Chlamydomonas reinhardtii* that despite being incomplete functions to maintain and assemble cilia. This incomplete complex lacks the ARPC5 subunit. In yeast, deletion of any of the genes encoding Arp2/3 cause severe defects and even lethality, but these defects differ in severity depending on the complex members deleted, suggesting that the complex members have varying degrees of importance in Arp2/3 function (Winter, Choe, and Li 1999). Incomplete complexes have also been described for specific functions. Hybrid Arp2/3 complexes that have vinculin and α-actinin substituted for ARPC1, ARPC4, and ARPC5 have been found to be important in focal adhesion formation (Chorev et al. 2014). Complexes containing only Arp2, Arp3, ARPC2, and ARPC4 are needed for invasion of *Listeria*, while complexes lacking only ARPC5 were required for comet tail formation (Kühbacher et al. 2015). This suggests not only that the complex can function lacking ARPC5 and other subunits, but that different combinations of subunits form Arp2/3 complexes that are required for different functions in the same overall process.

The role of ARPC5 in actin nucleation is being investigated by various groups. This subunit is potentially important for the association of ARPC1 to the complex, but a complex lacking ARPC5 can nucleate filaments and is able to cross-link (Gournier et al. 2001). More recent work suggests that ARPC5 is present primarily to regulate nucleation activity, as substituting isoforms of ARPC5 causes the nucleation activity to vary (von Loeffelholz et al. 2020). Thus, we believe that the lack of ARPC5 in this complex does not render it inactive. Furthermore, the data suggest that knocking out function of the Arp2/3 complex genetically or chemically does result in phenotypes, including altered mid-cell actin networks, defects in endocytosis, and problems with ciliary assembly and maintenance (**Figures 2-8**). However, it is not clear whether there is actually a 6-member complex in *Chlamydomonas* or whether a highly divergent ARPC5 exists because the overall homology of the Arp2/3 complex in *Chlamydomonas* is not high. Specifically, ARPC5 is thought to interact with ARPC4, which has 50% sequence identity compared to mammalian ARPC4, and with ARPC1, which has only 30% sequence identity compared to mammalian ARPC1B (**Figure 1A**). Further, we have yet to determine if the Arp2/3 complex of *Chlamydomonas* is able to nucleate branched or dendritic actin networks like conventional Arp2/3 complexes.

We do find the Arp2/3 loss disrupts actin localization in the cell, and that cells lacking a functional Arp2/3 complex have a more compact centrally located filamentous actin signal. This may be due to an increase in formin or bundler activity in the absence of Arp2/3. It has been proposed that actin binding proteins compete for a monomer pool (Christensen et al. 2017; Suarez and Kovar 2016). In the absence of Arp2/3-nucleated actin filaments, the competition for monomers is decreased allowing formin-mediated polymerization to increase. Additionally, the less spread out actin signal may indicate that the actin required for Golgi-independent trafficking is unavailable. Further, the accumulation of actin filaments near the Golgi in these cells may suggest Golgi-dependent trafficking is compensating for the loss of protein and membrane from other places. Additionally, in the cells lacking the Arp2/3 complex, we see a

near-complete loss of actin patches or dots that are reminiscent of endocytic patches seen in yeast. This suggests Arp2/3 is required for some sort of membrane remodeling occurring at the periphery of the cell.

A membrane protein internalization-requiring mechanism was reported in *Chlamydomonas* where relocalization of the known ciliary protein SAG1 from the periphery of the cell to the apex and ciliary region occurs (Belzile et al. 2013). Here, we show that this process is actin and Arp2/3-dependent. Because actin and Arp2/3 are required for endocytosis in other cells, this supports the possibility that endocytosis is happening in *Chlamydomonas*. We have also shown that while wild-type cells readily endocytose membrane dyes, the *arpc4* mutant does so less efficiently. This is further supported by the presence of the important clathrin-mediated endocytosis genes found in *Chlamydomonas.*

Finally, we find that Arp2/3 mediates ciliary assembly and maintenance in these cells. Ciliary assembly depends on incorporation of existing protein and membrane as well as synthesis and trafficking of new protein. Here, we have not ruled out that synthesis and trafficking of new protein are altered by Arp2/3 inhibition. However, the slow initial regeneration of cilia, which is likely utilizing existing proteins, and the almost complete lack of growth when new protein synthesis is blocked in Arp2/3-deficient cells suggests a model where Arp2/3 is required for the incorporation of existing ciliary components. We hypothesize that this is due to a problem with reclaiming of membrane and membrane protein from the plasma membrane, but we have also not yet ruled out defects in the size of the pool containing pre-existing proteins for ciliary assembly and maintenance. Any of these may be the cause of the assembly problems seen in the *arpc4* mutants, but as actin is widely functioning in the cell these causes are not mutually exclusive. In addition to the problems we see in ciliary assembly in *arpc4* mutants, collapsing the Golgi with BFA causes cells lacking Arp2/3 to resorb their cilia faster. In other words, cells with functioning Arp2/3 complexes are able to maintain their cilia from other sources of protein and membrane, supporting a role for Arp2/3 in membrane and membrane protein recruitment from the plasma membrane.

Three models for the trafficking of membrane proteins to cilia have been proposed: 1) Golgi vesicles containing ciliary proteins are docked at the base of the cilium and fuse with the ciliary membrane inside the cilium itself; 2) Golgi vesicles containing ciliary proteins are docked near the base of the cilium still within the diffusion barrier; and 3) Golgi vesicles containing proteins fuse with the plasma membrane barrier and membrane proteins are then somehow moved across this barrier within the plasma membrane (Nachury, Seeley, and Jin 2010). Based on the data presented here, we propose a fourth model for the recruitment of a reservoir of membrane proteins to the cilium. We hypothesize that ciliary membrane proteins targeted to the plasma membrane of the cell outside the diffusion barrier can be endocytosed and trafficked to cilia, either within or outside of the diffusion barrier in an actin and Arp2/3 dependent manner. An endocytic mechanism of trafficking in ciliogenesis has been investigated previously in mammalian cells. The ciliary pocket found at the base of primary and motile cilia has been found to be an endocytically active region (Molla-Herman et al. 2010). Many endocytosis genes have been found to be involved in ciliogenesis, and in fact, in *Chlamydomonas*, clathrin heavy chain has been found to localize at the base of cilia (Kaplan et al. 2012). Even in *Chlamydomonas*, it has been shown that plasma membrane surface-exposed proteins are relocalized to cilia during ciliary regeneration (W. Dentler 2013). Additionally, the

BBsome complex (Bardet Biedl Syndrome complex), which is involved in regulation of ciliary membrane protein composition, has been shown to interact with clathrin itself at the ciliary pocket to facilitate membrane sorting (Langousis et al. 2016), and in fact, some BBsome complex members resemble coat proteins such as clathrin (Jin et al. 2010).

Altogether, this leads us to hypothesize that the role Arp2/3 plays in ciliary assembly is related to an endocytic-dependent recruitment of a ciliary protein reservoir in the plasma membrane, particularly at the initial stages of ciliogenesis before Golgi-derived membrane and newly synthesized protein are required (**Figure 9**).

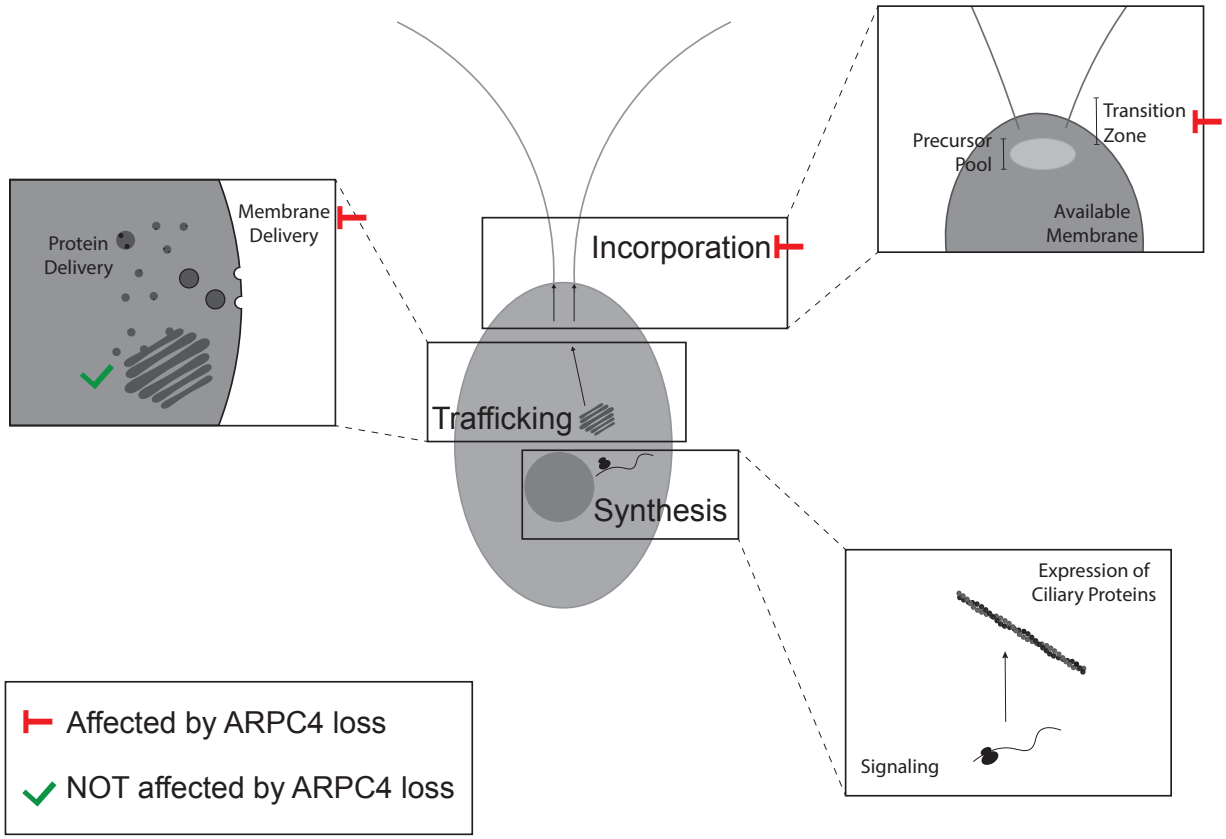

Figure 9. Arp2/3 is required for membrane and protein delivery via a Golgi-independent, endocytosis-like process. Model showing steps of ciliogenesis mediated by the Arp2/3 complex. These steps include incorporation of existing proteins and membrane, transition zone organization, and membrane delivery via an endocytic route as indicated by red symbols. Green symbols show steps of ciliogenesis not believed to be affected by Arp2/3.

METHODS

Strains:

The wild-type *Chlamydomonas* strain (CC-5325), the *arpc4* mutant (LMJ.RY0402.232713), the IDA5 mutant (CC-3420), and the NPHP4-HA strain (CC-5115) are from the *Chlamydomonas* resource center. The *nap1* mutant was a gift from Fred Cross, Masayuki Onishi, and John Pringle. The SAG1-HA strain was a gift from William Snell. Cells were grown and maintained on 1.5% Tris-Acetate Phosphate Agar (TAP) plates under constant blue (450- 475 nm) and red light

(625-660 nm). For experiments, cells were grown in liquid TAP media overnight under constant red and blue light with agitation from a rotator. To induce gametes for mating for the SAG1-HA experiments, cells were grown in liquid M-N media overnight with constant red and blue light and agitation.

Homology modeling and sequence studies:
Arp2/3 homology model was created using the Modeller plugin in UCSF Chimera. The template used was 1U2Z (Nolen, Littlefield, and Pollard 2004; Sali and Blundell 1993; Pettersen et al. 2004). Percent identity and similarity is calculated in relation to the human Arp2/3 complex members. Conservation map of the *Chlamydomonas* actins is based on the sequence alignment between IDA5, NAP1, and human actin generated in Geneious using MUSCLE. The regions of actin that bind ARPC2/ARPC4 were determined previously (Goley et al. 2010). Swiss-model was used to generate a homology model of IDA5 based on the structure PDB 2ZWH (Waterhouse et al. 2018; Oda et al. 2009). The homology model was visualized and conservation was mapped on the protein surface using Chimera (Pettersen et al. 2004).

Ciliary studies:
For steady state experiments, cells were treated with specified drugs (either 100μM CK-666, 250μM CK-666, 250μM CK-689, 10μM LatB, 10μM CHX, or 36μM BFA) and incubated with agitation for the allotted times. Following any incubation (as well as a pre sample) cells were diluted in an equal volume of 2% glutaraldehyde and incubated at 4 degrees until they sediment. Following sedimentation, cells were imaged using a Zeiss DIC scope with a 40X objective. Cilia were then measured using the segmented line function in ImageJ.

For regeneration experiments, a pre sample was taken by adding cells to an equal volume of 2% glutaraldehyde. Then cells were deciliated with 115μL of 0.5N acetic acid for 45 seconds. After this short incubation, the pH was returned to normal by adding 120μL of 0.5N KOH. A 0 sample was again taken by adding cells to an equal volume of 2% glutaraldehyde. Then cells were incubated with agitation and allowed to regrow cilia for the allotted time period with samples taken at the indicated time points by adding cells to an equal volume of 2% glutaraldehyde. Cells in glutaraldehyde were allowed to incubate at 4 degrees until sedimentation. Then, cells were imaged using the same Zeiss DIC scope with a 40X objective. Cilia were then measured using the segmented line function in ImageJ. (Jack and Avasthi 2018; Paul A. Lefebvre 1995)

Phalloidin staining and quantification:
Cells were mounted onto poly-lysine coverslips and fixed with fresh 4% paraformaldehyde in 1X HEPES. Coverslips with cells were then permeabilized with acetone and allowed to dry. Cells were rehydrated with PBS, stained with atto-phalloidin-488, and finally washed with PBS and allowed to dry before mounting with Fluoromount-G (Craig et al. 2019). Cells were then imaged using Nikon Spinning Disk Confocal. Z-stacks were obtained, and in ImageJ, sum projections were created for quantification purposes, while maximum intensity projections were created for viewing. Using sum slices in ImageJ, lines were drawn for line scans from the apex of the cell between cilia to furthest away basal position. Line scans were then normalized to each other

and background was subtracted. A gaussian curve was fit to each scan for full width at half max quantification.

Next, images in ImageJ were thresholded to the point to where either the whole cell was visible or just the mid-cell actin was visible. From these thresholded images, the area of the particle was obtained as well as the mean intensity and integrated density. The area of the mid-cell actin signal was divided by the area of the full cell to give a ratio. The mid-cell intensity was taken by using the mean signal and subtracting the background. The background corrected total cell fluorescence was calculated by taking the integrated density and subtracting the sum of the area and the background mean intensity.

NPHP4 Immunofluorescence:
Cells grown overnight in TAP medium were treated with either 10μM of LatB, 250μM of CK-666, or both. A pre sample, a 30-minute treatment sample, and a 2-hour treatment sample were adhered to poly-lysine coated coverslips. These cells were then fixed and permeabilized with methanol and allowed to dry. Cells were rehydrated with PBS and incubated with 100% block (1% BSA, 3% fish gelatin) for 30 minutes. The 100% block was replaced with new 100% block containing 10% normal goat serum for another 30-minute incubation. The primary antibody (rat anti-HA, Sigma) was diluted 1:1000 in 20% block in PBS. Coverslips were incubated at 4 degrees in a humidified chamber overnight. The primary antibody was then removed and washed away with 3 10-minute PBS washes. The secondary (anti-rat IgG-Alexafluor 488) was added and coverslips were incubated at room temperature for 1 hour. This was followed by 3 more 10-minute PBS washes and finally mounting with Fluoromount-G. Cells were imaged using a Nikon widefield microscope. Z-stacks were obtained, and maximum intensity projections were created using ImageJ and the presence or absence of dots was noted.

Electron microscopy:
Cells (1mL of each strain) were deciliated via pH shock by adding 115μL of 0.5N acetic acid for 45 seconds followed by 120μL of 0.5N KOH to bring cells back to neutral pH. Cells were allowed to regrow cilia for 30 minutes. A pre sample and a 30-minute post-deciliation sample were fixed in an equal volume of 2% glutaraldehyde for 20 minutes at room temperature. Samples were then pelleted using gentle centrifugation for 10 minutes. The supernatant was removed, and cells were resuspended in 1% glutaraldehyde, 20mM sodium cacodylate. Cells were incubated for 1 hour at room temperature and then overnight at 4 degrees. The staining protocol was first described in (W. L. Dentler and Adams 1992).

SAG1-HA Immunofluorescence:
SAG1-HA cells were grown overnight in M-N media to induce gametes. These cells are then treated with either 10μM LatB for 1 hour or 250μM CK-666 for 2 hours. Following treatment mating induction is done by adding db-cAMP to a final concentration of 13.5mM and incubating for 30 minutes. Cells are then adhered to coverslips and fixed with methanol. Cells were then dried and rehydrated with PBS and incubated with 100% block (5% BSA, 1% fish gelatin) for 30 minutes. The 100% block was replaced with new 100% block containing 10% normal goat serum for another 30-minute incubation. The primary antibody (rat anti-HA, Sigma) was diluted

1:1000 in 20% block in PBS. Coverslips were incubated at 4 degrees in a humidified chamber overnight. The primary antibody was removed and washed away with 3 10-minute PBS washes. The secondary (anti-rat IgG-Alexafluor 488) was added and coverslips were incubated at room temperature for 1 hour. This was followed by 3 more 10-minute PBS washes and finally mounting with Fluoromount-G. Cells were imaged using a Nikon widefield microscope. Z-stacks were obtained, and maximum intensity projections were created for visualization and sum slices were created for quantification using ImageJ.

Images were quantified by using line scans from the apex of the cells to the basal region of the cells farthest away from the apex. Line scans were then normalized, and background subtracted before being combined into single graphs. Using the line scans, the intensity of signal at the basal region of the cells was subtracted from the signal at the apical region. Finally, cells with a difference over 30 were considered to be apically enriched and this was quantified as percentage of cells with apical staining.

SAG1-HA western blot:
SAG1-HA cells were grown overnight in M-N media to induce gametes. These cells are then treated with either 10μM LatB for 1 hour or 250μM CK-666 for 2 hours. Following treatment mating induction is done by adding db-cAMP to a final concentration of 13.5mM and incubating for 10 minutes. Cells were then treated with 0.01% trypsin for 5 minutes. Cells were then pelleted (at 500xg for 2 minutes), resuspended in lysis buffer (5% glycerol, 1% NP-40, 1mM DTT, 1X protease inhibitors), and then lysed with bead beating. Cell debris was spun down at 14000rpm for 15 minutes. An equal amount of protein was loaded to a 10% SDS-PAGE gel. The resulting gel was transferred to membrane which was then blocked with 5% milk in PBST. The primary antibody (rabbit anti-HA, cell signaling) diluted to 1:1000 in 1% BSA, 1% milk was added and incubated overnight at 4 degrees. Primary antibody washed off with 3 10-minute PBST washes. Secondary antibody (anti rabbit IgG, cell signaling) diluted 1:5000 in 1% milk, 1% BSA was added and the blot was incubated for 1 hour. Membrane was probed with West Pico Chemiluminescent Pico Substrate. Total protein was determined with amido black staining. Band intensity was measured in ImageJ and normalized to total protein

Membrane stain:
FM 4-64FX membrane stain (Thermo) was diluted to a stock concentration of 200ug/mL. Cells were adhered to poly-lysine coverslips. After a 5-minute incubation, cells were tilted off and 5ug/mL of ice-cold stain in Hank's Buffered Salt Solution (HBSS) without magnesium or calcium was added for 1 minute. The stain was tilted off and cells were fixed with ice cold 4% paraformaldehyde in HBSS without magnesium or calcium for 15 minutes. Coverslips were then rinsed 3 times for 10 minutes each in ice cold HBSS without magnesium or calcium. Finally, cells were mounted with Fluoromount-G and imaged using the Nikon Spinning Disk Confocal. Z-stacks were taken and combined into sum projections using ImageJ. The background corrected total cell fluorescence was then calculated by taking the integrated density and subtracting the sum of the area and the mean background intensity.

ACKNOWLEDGEMENTS:

Our most sincere gratitude to William Dentler for providing his expertise especially in looking at the electron microscopy images and for his helpful advice, William Snell for generously providing the SAG1-HA strain, Masayuki Onishi for generously providing the *nap1* mutant strain, Henry Higgs for his feedback on the manuscript, Ann Lavanway for assistance with microscopy, and the Avasthi lab for all their help throughout the project.

We also thank our funding sources including the Madison and Lila Self Graduate Fellowship at the University of Kansas Medical Center, the MIRA (R35GM128702), the Jane Coffin Childs Memorial Fund, and the National Institute of General Medicine Science (1K99GM137038-01). Finally, we thank the BioMT core at Dartmouth College (NIH/NIGMS COBRE award P20-GM113132) and the KIDDRC NIH U54 HD 090216 at the University of Kansas Medical Center, Kansas City, KS 66160.

REFERENCES:

Adams, A E, and J R Pringle. 1984. "Relationship of Actin and Tubulin Distribution to Bud Growth in Wild-Type and Morphogenetic-Mutant Saccharomyces Cerevisiae." *Journal of Cell Biology* 98 (3): 934–45. https://doi.org/10.1083/jcb.98.3.934.

Aghamohammadzadeh, Soheil, and Kathryn R. Ayscough. 2009. "Differential Requirements for Actin during Yeast and Mammalian Endocytosis." *Nature Cell Biology* 11 (8): 1039–42. https://doi.org/10.1038/ncb1918.

Avasthi, Prachee, Masayuki Onishi, Joel Karpiak, Ryosuke Yamamoto, Luke Mackinder, Martin C Jonikas, Winfield S Sale, Brian Shoichet, John R Pringle, and Wallace F Marshall. 2014. "Actin Is Required for IFT Regulation in Chlamydomonas Reinhardtii." *Current Biology* 24 (17): 2025–32. https://doi.org/10.1016/j.cub.2014.07.038.

Awata, Junya, Saeko Takada, Clive Standley, Karl F. Lechtreck, Karl D. Bellvé, Gregory J. Pazour, Kevin E. Fogarty, and George B. Witman. 2014. "NPHP4 Controls Ciliary Trafficking of Membrane Proteins and Large Soluble Proteins at the Transition Zone." *Journal of Cell Science* 127 (Pt 21): 4714–27. https://doi.org/10.1242/jcs.155275.

Ayscough, K. R., J. Stryker, N. Pokala, M. Sanders, P. Crews, and D. G. Drubin. 1997. "High Rates of Actin Filament Turnover in Budding Yeast and Roles for Actin in Establishment and Maintenance of Cell Polarity Revealed Using the Actin Inhibitor Latrunculin-A." *The Journal of Cell Biology* 137 (2): 399–416. https://doi.org/10.1083/jcb.137.2.399.

Basu, Roshni, Emilia Laura Munteanu, and Fred Chang. 2014. "Role of Turgor Pressure in Endocytosis in Fission Yeast." *Molecular Biology of the Cell* 25 (5): 679–87. https://doi.org/10.1091/mbc.E13-10-0618.

Belzile, Olivier, Carmen I Hernandez-Lara, Qian Wang, and William J Snell. 2013. "Regulated Membrane Protein Entry into Flagella Is Facilitated by Cytoplasmic Microtubules and Does Not Require IFT." *Current Biology : CB* 23 (15): 1460–65. https://doi.org/10.1016/j.cub.2013.06.025.

Campellone, K., and M. Welch. 2010. "A Nucleator Arms Race: Cellular Control of Actin Assembly." *Nature Reviews Molecular Cell Biology* 11: 237–51.

Carlsson, Anders E., and Philip V. Bayly. 2014. “Force Generation by Endocytic Actin Patches in Budding Yeast.” *Biophysical Journal* 106 (8): 1596–1606. https://doi.org/10.1016/j.bpj.2014.02.035.

Cheng, Xi, Gai Liu, Wenting Ke, Lijuan Zhao, Bo Lv, Xiaocui Ma, Nannan Xu, et al. 2017. “Building a Multipurpose Insertional Mutant Library for Forward and Reverse Genetics in Chlamydomonas.” *Plant Methods* 13 (1): 36. https://doi.org/10.1186/s13007-017-0183-5.

Chorev, Dror S., Oren Moscovitz, Benjamin Geiger, and Michal Sharon. 2014. “Regulation of Focal Adhesion Formation by a Vinculin-Arp2/3 Hybrid Complex.” *Nature Communications* 5 (1): 3758. https://doi.org/10.1038/ncomms4758.

Christensen, J. R., G. M. Hocky, K. E. Homa, A. N. Morganthaler, S. E. Hitchcock-DeGregori, G. A. Voth, and D. R. Kovar. 2017. “Competition between Tropomyosin, Fimbrin, and ADF/Cofilin Drives Their Sorting to Distinct Actin Filament Networks.” *Elife* 6 (March). https://doi.org/10.7554/eLife.23152.

Craig, Evan W., David M. Mueller, Brae M. Bigge, Miroslava Schaffer, Benjamin D. Engel, and Prachee Avasthi. 2019. “The Elusive Actin Cytoskeleton of a Green Alga Expressing Both Conventional and Divergent Actins.” *Molecular Biology of the Cell*, mbc.E19-03-0141. https://doi.org/10.1091/mbc.E19-03-0141.

Dentler, W L, and C Adams. 1992. “Flagellar Microtubule Dynamics in Chlamydomonas: Cytochalasin D Induces Periods of Microtubule Shortening and Elongation; and Colchicine Induces Disassembly of the Distal, but Not Proximal, Half of the Flagellum.” *The Journal of Cell Biology* 117 (6): 1289–98. https://doi.org/10.1083/jcb.117.6.1289.

Dentler, William. 2013. “A Role for the Membrane in Regulating Chlamydomonas Flagellar Length.” *PLOS ONE* 8 (1): e53366. https://doi.org/10.1371/journal.pone.0053366.

Diener, Dennis R, Pietro Lupetti, and Joel L Rosenbaum. 2015. “Proteomic Analysis of Isolated Ciliary Transition Zones Reveals the Presence of ESCRT Proteins.” *Current Biology : CB* 25 (3): 379–84. https://doi.org/10.1016/j.cub.2014.11.066.

Farina, Francesca, Jérémie Gaillard, Christophe Guérin, Yohann Couté, James Sillibourne, Laurent Blanchoin, and Manuel Théry. 2016. “The Centrosome Is an Actin-Organizing Centre.” *Nature Cell Biology* 18 (1): 65–75. https://doi.org/10.1038/ncb3285.

Goley, Erin D., Aravind Rammohan, Elizabeth A. Znameroski, Elif Nur Firat-Karalar, David Sept, and Matthew D. Welch. 2010. “An Actin-Filament-Binding Interface on the Arp2/3 Complex Is Critical for Nucleation and Branch Stability.” *Proceedings of the National Academy of Sciences* 107 (18): 8159. https://doi.org/10.1073/pnas.0911668107.

Goode, Bruce L, Julian A Eskin, and Beverly Wendland. 2015. “Actin and Endocytosis in Budding Yeast.” *Genetics* 199 (2): 315–58. https://doi.org/10.1534/genetics.112.145540.

Gournier, Helene, Erin D. Goley, Hanspeter Niederstrasser, Thong Trinh, and Matthew D. Welch. 2001. “Reconstitution of Human Arp2/3 Complex Reveals Critical Roles of Individual Subunits in Complex Structure and Activity.” *Molecular Cell* 8 (5): 1041–52. https://doi.org/10.1016/S1097-2765(01)00393-8.

Hetrick, Byron, Min Suk Han, Luke A Helgeson, and Brad J Nolen. 2013. “Small Molecules CK-666 and CK-869 Inhibit Actin-Related Protein 2/3 Complex by Blocking an Activating Conformational Change.” *Chemistry & Biology* 20 (5): 701–12. https://doi.org/10.1016/j.chembiol.2013.03.019.

Hirono, Masafumi, Satomi Uryu, Akio Ohara, Takako Kato-Minoura, and Ritsu Kamiya. 2003. "Expression of Conventional and Unconventional Actins in Chlamydomonas Reinhardtii upon Deflagellation and Sexual Adhesion." *Eukaryotic Cell* 2 (3): 486–93. https://doi.org/10.1128/ec.2.3.486-493.2003.

Inoue, Daisuke, Dorian Obino, Judith Pineau, Francesca Farina, Jérémie Gaillard, Christophe Guerin, Laurent Blanchoin, Ana-Maria Lennon-Duménil, and Manuel Théry. 2019. "Actin Filaments Regulate Microtubule Growth at the Centrosome." *The EMBO Journal* 38 (11). https://doi.org/10.15252/embj.201899630.

Jack, Brittany, and Prachee Avasthi. 2018. "Erratum to: Chemical Screening for Flagella-Associated Phenotypes in Chlamydomonas Reinhardtii." *Methods in Molecular Biology (Clifton, N.J.)* 1795: E1. https://doi.org/10.1007/978-1-4939-7874-8_19.

Jack, Brittany, David M. Mueller, Ann C. Fee, Ashley L. Tetlow, and Prachee Avasthi. 2019. "Partially Redundant Actin Genes in Chlamydomonas Control Transition Zone Organization and Flagellum-Directed Traffic." *Cell Reports* 27 (8): 2459-2467.e3. https://doi.org/10.1016/j.celrep.2019.04.087.

Jin, Hua, Susan Roehl White, Toshinobu Shida, Stefan Schulz, Mike Aguiar, Steven P. Gygi, J. Fernando Bazan, and Maxence V. Nachury. 2010. "The Conserved Bardet-Biedl Syndrome Proteins Assemble a Coat That Traffics Membrane Proteins to Cilia." *Cell* 141 (7): 1208–19. https://doi.org/10.1016/j.cell.2010.05.015.

Kaplan, Oktay I., David B. Doroquez, Sebiha Cevik, Rachel V. Bowie, Lara Clarke, Anna A.W.M. Sanders, Katarzyna Kida, Joshua Z. Rappoport, Piali Sengupta, and Oliver E. Blacque. 2012. "Endocytosis Genes Facilitate Protein and Membrane Transport in C. Elegans Sensory Cilia." *Current Biology* 22 (6): 451–60. https://doi.org/10.1016/j.cub.2012.01.060.

Kato, T., O. Kagami, T. Yagi, and R. Kamiya. 1993. "Isolation of Two Species of Chlamydomonas Reinhardtii Flagellar Mutants, Ida5 and Ida6, That Lack a Newly Identified Heavy Chain of the Inner Dynein Arm." *Cell Structure and Function* 18 (6): 371–77. https://doi.org/10.1247/csf.18.371.

Kato-Minoura, T, M Hirono, and R Kamiya. 1997. "Chlamydomonas Inner-Arm Dynein Mutant, Ida5, Has a Mutation in an Actin-Encoding Gene." *The Journal of Cell Biology* 137 (3): 649–56. https://doi.org/10.1083/jcb.137.3.649.

Kato-Minoura, T, S Uryu, M Hirono, and R Kamiya. 1998. "Highly Divergent Actin Expressed in a Chlamydomonas Mutant Lacking the Conventional Actin Gene." *Biochemical and Biophysical Research Communications* 251 (1): 71–76. https://doi.org/10.1006/bbrc.1998.9373.

Kiesel, Petra, Gonzalo Alvarez Viar, Nikolai Tsoy, Riccardo Maraspini, Peter Gorilak, Vladimir Varga, Alf Honigmann, and Gaia Pigino. 2020. "The Molecular Structure of Mammalian Primary Cilia Revealed by Cryo-Electron Tomography." *Nature Structural & Molecular Biology*, September. https://doi.org/10.1038/s41594-020-0507-4.

Kim, Joon, Ji Eun Lee, Susanne Heynen-Genel, Eigo Suyama, Keiichiro Ono, Kiyoung Lee, Trey Ideker, Pedro Aza-Blanc, and Joseph G. Gleeson. 2010. "Functional Genomic Screen for Modulators of Ciliogenesis and Cilium Length." *Nature* 464 (7291): 1048–51. https://doi.org/10.1038/nature08895.

Kühbacher, Andreas, Mario Emmenlauer, Pauli Rämo, Natasha Kafai, Christoph Dehio, Pascale Cossart, and Javier Pizarro-Cerdá. 2015. “Genome-Wide SiRNA Screen Identifies Complementary Signaling Pathways Involved in Listeria</Em> Infection and Reveals Different Actin Nucleation Mechanisms during Listeria</Em> Cell Invasion and Actin Comet Tail Formation.” Edited by Julian E. Davies. *MBio* 6 (3): e00598-15. https://doi.org/10.1128/mBio.00598-15.

Langousis, Gerasimos, Michelle M. Shimogawa, Edwin A. Saada, Ajay A. Vashisht, Roberto Spreafico, Andrew R. Nager, William D. Barshop, Maxence V. Nachury, James A. Wohlschlegel, and Kent L. Hill. 2016. “Loss of the BBSome Perturbs Endocytic Trafficking and Disrupts Virulence of Trypanosoma Brucei.” *Proceedings of the National Academy of Sciences of the United States of America* 113 (3): 632–37. https://doi.org/10.1073/pnas.1518079113.

Lefebvre, P. A., S. A. Nordstrom, J. E. Moulder, and J. L. Rosenbaum. 1978. “Flagellar Elongation and Shortening in Chlamydomonas. IV. Effects of Flagellar Detachment, Regeneration, and Resorption on the Induction of Flagellar Protein Synthesis.” *The Journal of Cell Biology* 78 (1): 8–27. https://doi.org/10.1083/jcb.78.1.8.

Lefebvre, Paul A. 1995. “Flagellar Amputation and Regeneration in Chlamydomonas.” In *Methods in Cell Biology*, 47:3–7. Elsevier.

Li, Xiaobo, Weronika Patena, Friedrich Fauser, Robert E. Jinkerson, Shai Saroussi, Moritz T. Meyer, Nina Ivanova, et al. 2019. “A Genome-Wide Algal Mutant Library and Functional Screen Identifies Genes Required for Eukaryotic Photosynthesis.” *Nature Genetics* 51 (4): 627–35. https://doi.org/10.1038/s41588-019-0370-6.

Loeffelholz, Ottilie von, Andrew Purkiss, Luyan Cao, Svend Kjaer, Naoko Kogata, Guillaume Romet-Lemonne, Michael Way, and Carolyn A. Moores. 2020. “Cryo-EM of Human Arp2/3 Complexes Provides Structural Insights into Actin Nucleation Modulation by ARPC5 Isoforms.” *BioRxiv*, January, 2020.05.01.071704. https://doi.org/10.1101/2020.05.01.071704.

Molla-Herman, Anahi, Rania Ghossoub, Thierry Blisnick, Alice Meunier, Catherine Serres, Flora Silbermann, Chris Emmerson, et al. 2010. “The Ciliary Pocket: An Endocytic Membrane Domain at the Base of Primary and Motile Cilia.” *Journal of Cell Science* 123 (Pt 10): 1785–95. https://doi.org/10.1242/jcs.059519.

Nachury, Maxence V., E. Scott Seeley, and Hua Jin. 2010. “Trafficking to the Ciliary Membrane: How to Get across the Periciliary Diffusion Barrier?” *Annual Review of Cell and Developmental Biology* 26: 59–87. https://doi.org/10.1146/annurev.cellbio.042308.113337.

Nolen, Brad J., Ryan S. Littlefield, and Thomas D. Pollard. 2004. “Crystal Structures of Actin-Related Protein 2/3 Complex with Bound ATP or ADP.” *Proceedings of the National Academy of Sciences of the United States of America* 101 (44): 15627. https://doi.org/10.1073/pnas.0407149101.

Oda, Toshiro, Mitsusada Iwasa, Tomoki Aihara, Yuichiro Maéda, and Akihiro Narita. 2009. “The Nature of the Globular- to Fibrous-Actin Transition.” *Nature* 457 (7228): 441–45. https://doi.org/10.1038/nature07685.

Onishi, M., K. Pecani, T. th Jones, J. R. Pringle, and F. R. Cross. 2018. “F-Actin Homeostasis through Transcriptional Regulation and Proteasome-Mediated Proteolysis.” *Proc Natl Acad Sci U S A* 115 (28): E6487-e6496. https://doi.org/10.1073/pnas.1721935115.

Onishi, M., J. R. Pringle, and F. R. Cross. 2016. “Evidence That an Unconventional Actin Can Provide Essential F-Actin Function and That a Surveillance System Monitors F-Actin Integrity in Chlamydomonas.” *Genetics* 202 (3): 977–96. https://doi.org/10.1534/genetics.115.184663.

Onishi, Masayuki, James G. Umen, Frederick R. Cross, and John R. Pringle. 2019. “Cleavage-Furrow Formation without F-Actin in Chlamydomonas</Em>.” *BioRxiv*, January, 789016. https://doi.org/10.1101/789016.

Park, Tae Joo, Brian J. Mitchell, Philip B. Abitua, Chris Kintner, and John B. Wallingford. 2008. “Dishevelled Controls Apical Docking and Planar Polarization of Basal Bodies in Ciliated Epithelial Cells.” *Nature Genetics* 40 (7): 871–79. https://doi.org/10.1038/ng.104.

Pasquale, S M, and U W Goodenough. 1987. “Cyclic AMP Functions as a Primary Sexual Signal in Gametes of Chlamydomonas Reinhardtii.” *The Journal of Cell Biology* 105 (5): 2279–92. https://doi.org/10.1083/jcb.105.5.2279.

Pedersen, Lotte B., and Joel L. Rosenbaum. 2008. “Intraflagellar Transport (IFT) Role in Ciliary Assembly, Resorption and Signalling.” *Current Topics in Developmental Biology* 85: 23–61. https://doi.org/10.1016/S0070-2153(08)00802-8.

Pettersen, Eric F., Thomas D. Goddard, Conrad C. Huang, Gregory S. Couch, Daniel M. Greenblatt, Elaine C. Meng, and Thomas E. Ferrin. 2004. “UCSF Chimera--a Visualization System for Exploratory Research and Analysis.” *Journal of Computational Chemistry* 25 (13): 1605–12. https://doi.org/10.1002/jcc.20084.

Robinson, Robert C., Kirsi Turbedsky, Donald A. Kaiser, Jean-Baptiste Marchand, Henry N. Higgs, Senyon Choe, and Thomas D. Pollard. 2001. “Crystal Structure of Arp2/3 Complex.” *Science* 294 (5547): 1679. https://doi.org/10.1126/science.1066333.

Rohatgi, Rajat, and William J Snell. 2010. “The Ciliary Membrane.” *Current Opinion in Cell Biology* 22 (4): 541–46. https://doi.org/10.1016/j.ceb.2010.03.010.

Rosenbaum, J. L., J. E. Moulder, and D. L. Ringo. 1969. “Flagellar Elongation and Shortening in Chlamydomonas. The Use of Cycloheximide and Colchicine to Study the Synthesis and Assembly of Flagellar Proteins.” *The Journal of Cell Biology* 41 (2): 600–619. https://doi.org/10.1083/jcb.41.2.600.

Sali, A., and T. L. Blundell. 1993. “Comparative Protein Modelling by Satisfaction of Spatial Restraints.” *Journal of Molecular Biology* 234 (3): 779–815. https://doi.org/10.1006/jmbi.1993.1626.

Spector, Ilan, Nava R. Shochet, Dina Blasberger, and Yoel Kashman. 1989. “Latrunculins—Novel Marine Macrolides That Disrupt Microfilament Organization and Affect Cell Growth: I. Comparison with Cytochalasin D.” *Cell Motility* 13 (3): 127–44. https://doi.org/10.1002/cm.970130302.

Suarez, C., and D. R. Kovar. 2016. “Internetwork Competition for Monomers Governs Actin Cytoskeleton Organization.” *Nat Rev Mol Cell Biol* 17 (12): 799–810. https://doi.org/10.1038/nrm.2016.106.

Szymanska, Katarzyna, and Colin A. Johnson. 2012. “The Transition Zone: An Essential Functional Compartment of Cilia.” *Cilia* 1 (1): 10. https://doi.org/10.1186/2046-2530-1-10.

Waterhouse, Andrew, Martino Bertoni, Stefan Bienert, Gabriel Studer, Gerardo Tauriello, Rafal Gumienny, Florian T Heer, et al. 2018. “SWISS-MODEL: Homology Modelling of Protein Structures and Complexes.” *Nucleic Acids Research* 46 (W1): W296–303. https://doi.org/10.1093/nar/gky427.

Wingfield, Jenna L, Ilaria Mengoni, Heather Bomberger, Yu-Yang Jiang, Jonathon D Walsh, Jason M Brown, Tyler Picariello, et al. 2017. “IFT Trains in Different Stages of Assembly Queue at the Ciliary Base for Consecutive Release into the Cilium.” Edited by Erwin J G Peterman. *ELife* 6 (May): e26609. https://doi.org/10.7554/eLife.26609.

Winter, D. C., E. Y. Choe, and R. Li. 1999. “Genetic Dissection of the Budding Yeast Arp2/3 Complex: A Comparison of the in Vivo and Structural Roles of Individual Subunits.” *Proceedings of the National Academy of Sciences of the United States of America* 96 (13): 7288–93. https://doi.org/10.1073/pnas.96.13.7288.

Wu, Chien-Ting, Hsin-Yi Chen, and Tang K. Tang. 2018. “Myosin-Va Is Required for Preciliary Vesicle Transportation to the Mother Centriole during Ciliogenesis.” *Nature Cell Biology* 20 (2): 175–85. https://doi.org/10.1038/s41556-017-0018-7.